XIV International Conference on Topics in Astroparticle and Underground Physics (TAUP 2015) IOP Publishing
Journal of Physics: Conference Series **718** (2016) 062052 doi:10.1088/1742-6596/718/6/062052

Low energy neutrinos in Super-Kamiokande

Hiroyuki Sekiya

Kamioka Observatory, Institute for Cosmic Ray Research, University of Tokyo, 456 Higashi-mozumi, Hida, Gifu, 506-1205, Japan

E-mail: sekiya@icrr.u-tokyo.ac.jp

Abstract. Super-Kamiokande (SK), a 50 kton water Cherenkov detector, observes ^{8}B solar neutrinos via neutrino-electron elastic scattering. The analysis threshold was successfully lowered to 3.5 MeV (recoil electron kinetic energy) in SK-IV. To date SK has observed solar neutrinos for 18 years. An analysis regarding possible correlations between the solar neutrino flux and the 11 year solar activity cycle is shown. With large statistics, SK searches for distortions of the solar neutrino energy spectrum caused by the MSW resonance in the core of the sun. SK also searches for a day/night solar neutrino flux asymmetry induced by the matter in the Earth.

The Super-Kamiokande Gd (SK-Gd) project is the upgrade of the SK detector via the addition of water-soluble gadolinium (Gd) salt. This modification will enable it to efficiently identify low energy anti-neutrinos. SK-Gd will pursue low energy physics currently inaccessible to SK due to backgrounds. The most important will be the world's first observation of the diffuse supernova neutrino background. The main R&D program towards SK-Gd is EGADS: a 200 ton, fully instrumented tank built in a new cavern in the Kamioka mine.

1. Solar Neutrinos

Solar neutrino flux measurements from Super-Kamiokande (SK) [1] and the Sudbury Neutrino Observatory(SNO) [2] have provided direct evidence for solar neutrino flavor conversion. However, there is still no clear evidence that this solar neutrino flavor conversion is indeed due to neutrino oscillations and not caused by any other mechanism. Currently there are two testable signatures unique to neutrino oscillations. The first is the observation and precision test of the MSW resonance curve [3]. Based on oscillation parameters extracted from solar neutrino and reactor anti-neutrino measurements, there is an expected characteristic energy dependence of the flavor conversion. The higher energy solar neutrinos (higher energy ^{8}B and hep neutrinos) undergo complete resonant conversion within the sun, while the flavor changes of the lower energy solar neutrinos (pp, ^{7}Be, pep, CNO and lower energy ^{8}B neutrinos) arise only from vacuum oscillations. The transition from the matter dominated oscillations within the sun, to the vacuum dominated oscillations, should occur near 3 MeV, making ^{8}B neutrinos the best choice when looking for a transition point within the energy spectrum. The second signature arises from the effect of the terrestrial matter density on solar neutrino oscillations. This effect is tested directly by comparing solar neutrinos which pass through the Earth at nighttime to those which do not during the daytime. Those neutrinos which pass through the Earth will in general have an enhanced electron neutrino content compared to those which do not, leading to an increase in the nighttime electron elastic scattering rate (or any charged-current interaction rate), and hence a negative "day/night asymmetry". SK detects ^{8}B solar neutrinos over a wide

energy range in real time, making it a prime detector to search for both solar neutrino oscillation signatures.

After installation of the new front-end electronics, SK-IV started on October 6, 2008 with the low energy threshold of 3.5 MeV. The SK-IV results presented here include data taken until March 31, 2015 (2034 days). The measured flux, $\Phi_{^8\mathrm{B}}$ through all SK phases is $\{2.341 \pm 0.044\} \times 10^6/\mathrm{cm}^2/\mathrm{sec}$. The solar activity cycle is the 11 years periodic change of sun spots releasing the magnetic flux at the surface of the Sun. They are strongly correlated with the solar activity cycle. As SK observed solar neutrinos for 18 years, about 1.5 solar activity cycles, an analysis regarding possible correlations between the solar neutrino flux and the solar activity cycle was conducted. Fig.1 shows the SK yearly flux measured throughout the different phases of SK together with the corresponding sun spot number. Using the present data, a constant flux was fitted and the χ^2 was calculated with total experimental error as $\chi^2 = 13.10/18$ d.o.f., which corresponds to a probability of 78.6%. SK solar rate measurements are fully consistent with a constant solar neutrino flux emitted by the Sun.

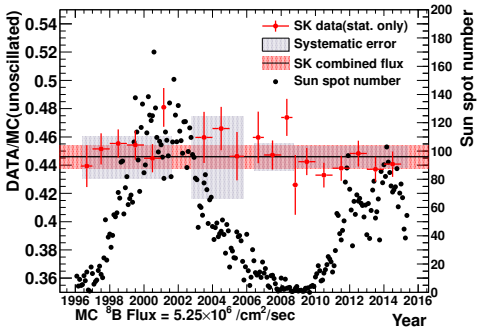

Figure 1. Solar neutrino yearly flux. The red points show the yearly flux measured by SK (statistical error only), the gray bands show the systematic error for each SK phase, the red band shows the error on the combined solar neutrino flux and the black points show the sun spot number.

The neutrino energy spectrum shape analysis utilized combined fits to SK-I, II, and III data as well as 1669 days of SK-IV data (until January 31 2014) with two generic functions as survival probability; $P_{ee}(E_\nu) = c_0 + c_1\left(\frac{E_\nu}{MeV} - 10\right) + c_2\left(\frac{E_\nu}{MeV} - 10\right)^2$ (quadratic) and $P_{ee}(E_\nu) = e_0 + \frac{e_1}{e_2}\left(\exp\left(e_2\left(\frac{E_\nu}{MeV} - 10\right)\right) - 1\right)$ (exponential). The fit takes correlations between SK phases and energy bins into account. The left of Fig.2 shows the energy spectrum measured by SK-IV which is expressed as the ratio of the observed elastic scattering rates over MC simulated expectation. Here, the ^{8}B flux was constrained by SNO's NC measurement [2]. The right of Fig.2 shows the statistical combination of the four phases of SK, along with the best-fit coming from the generic function fits. Also the expected MSW resonance curve assuming the best-fit neutrino oscillation parameters coming from a fit to SK data (all solar neutrino plus KamLAND data) is shown. SK spectrum results slightly disfavor the MSW resonance curves, but are consistent with the MSW resonance prediction within $1.0 - 1.7\sigma$.

The SK-IV livetime during the day (night) is 799.7 days (869.1 days). The solar neutrino flux between 4.5 and 19.5 MeV and assuming no oscillations is measured as $\Phi_D = (2.25 \pm 0.03(\mathrm{stat.}) \pm 0.38(\mathrm{sys.})) \times 10^6/(\mathrm{cm}^2\mathrm{sec})$ during the day and $\Phi_N = (2.36 \pm 0.03(\mathrm{stat.}) \pm 0.40(\mathrm{sys.})) \times 10^6/(\mathrm{cm}^2\mathrm{sec})$ during the night. A more sophisticated method to test the day/night effect is given in [4, 5]. For a given set of oscillation parameters, the interaction rate as a function of the solar zenith angle

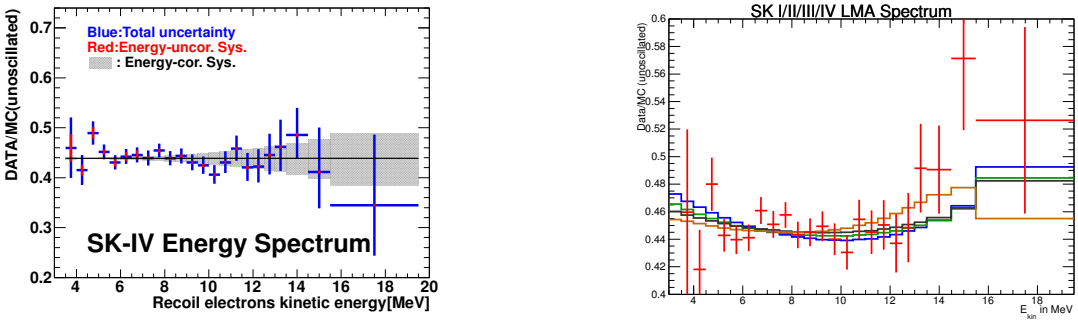

Figure 2. Left: The solar neutrino energy spectrum in SK-IV. Each point shows the ratio of the data to the expected flux using a non-oscillated ^{8}B solar neutrino spectrum. Right: The energy spectrum combining SK-I to SK-IV with prediction for (1)$\sin^2\theta_{12} = 0.308$ and $\Delta m^2_{21} = 7.50 \times 10^{-5}$ eV^2 (blue), (2)$\sin^2\theta_{12} = 0.311$ and $\Delta m^2_{21} = 4.85 \times 10^{-5}$ eV^2 (green), (3)quadratic fit (black) and (4)exponential fit (orange).

is predicted. Only the shape of the calculated solar zenith angle variation is used, the amplitude of it is scaled by an arbitrary parameter. The extended maximum likelihood fit to extract the solar neutrino signal is expanded to allow time-varying signals. The likelihood is then evaluated as a function of the average signal rates, the background rates and the scaling parameter which is called the "day/night amplitude". The equivalent day/night asymmetry is calculated by multiplying the fit scaling parameter with the expected day/night asymmetry. Because the amplitude fit depends on the assumed shape of the day/night variation, it necessarily depends on the oscillation parameters, although with very little dependence expected on the mixing angles

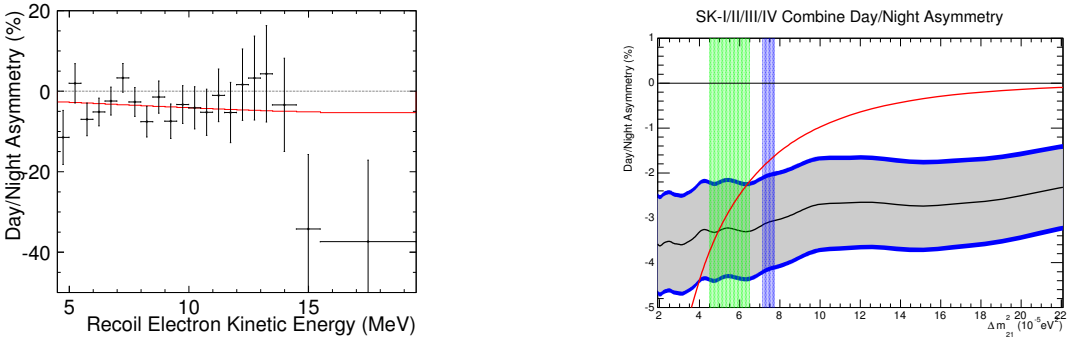

Figure 3. Left: SK combined energy dependence of the fitted day/night asymmetry (measured day/night amplitude times the expected asymmetry (red)) for $\Delta m^2_{21} = 4.84 \times 10^{-5}$eV^2, $\sin^2\theta_{12} = 0.311$ and $\sin^2\theta_{13} = 0.025$. The error bars shown are statistical uncertainties only. Right: Dependence of the measured day/night asymmetry (fitted day/night amplitude times the expected day/night asymmetry (red)) on Δm^2_{21} (light gray band=stat. error, dark gray band=stat.+syst. error) for $\sin^2\theta_{12} = 0.311$ and $\sin^2\theta_{13} = 0.025$. Overlaid are the allowed ranges from solar neutrino data (green band) and KamLAND (blue band).

The day/night asymmetry coming from the SK-I to IV combined amplitude fit can be seen as a function of recoil electron kinetic energy in the left of Fig.3, for $\Delta m^2_{21} = 4.84 \times 10^5$eV^2, $\sin^2\theta_{12} = 0.311$ and $\sin^2\theta_{13} = 0.025$. The right of Fig.3 shows the Δm^2_{21} dependence of the SK all phases combined day/night asymmetry for $\sin^2\theta_{12} = 0.311$ and $\sin^2\theta_{13} = 0.025$. The point

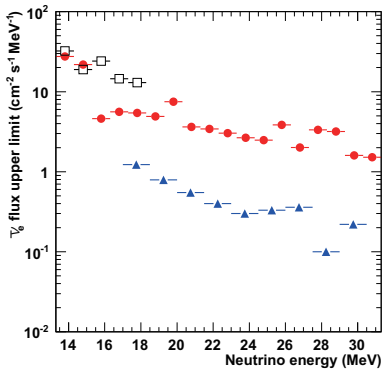

Figure 4. Model-independent SRN 90% C.L. upper limits as a function of neutrino energy for SK-IV (solid circle). For comparison, both KamLAND result (open square) and previous SK result (solid triangle) are also shown.

where the best fit crosses the expected curve represents the value of Δm^2_{21} where the measured day/night asymmetry is equal to the expectation. Superimposed are the allowed ranges in Δm^2_{21} from the global solar neutrino data fit (green) and from KamLAND (blue). The amplitude fit shows no dependence on the values of θ_{12} (within the LMA region of the MSW plane) or θ_{13}.

2. Super-Kamiokande Gd project

The Supernova Relic Neutrinos (SRNs) signal is the diffuse supernova neutrino background from all the supernovae in the past. The observation of SRNs in general or neutrinos from distant supernovae in particular, would give us some information about the universe, for example the core collapse rate from SRNs, and about the neutrino itself too, for example its lifetime. This signal has never been detected, but it is expected to be detectable in the 16-30 MeV energy region, which is the gap between the energy ranges of solar neutrinos and atmospheric neutrinos. SK-I, II and SK-III data were analyzed with energy threshold 16MeV [6]. A maximum likelihood search was performed in multiple regions of the Cherenkov angle distribution to extract the most accurate flux limit. The obtained flux limit is between 2.7 and 3.0 $\bar{\nu}cm^{-2}s^{-1}$ (positron energy $>$ 16 MeV), which actually depends on the shape of the neutrino spectrum assumed. This result currently provides the world's best limit on SRN flux. In SK-IV, a new result of the SRN search using the neutron tagging technique was also published [7]. In this analysis, neutrons from SRN reactions $(\bar{\nu_e}, p \rightarrow e^+, n)$ are captured by hydrogens. After neutron captures, 2.2 MeV gammas are emitted. Thus, by detecting the prompt positron signal and the delayed 2.2 MeV gamma signal, most of backgrounds which are not accompanied by neutrons can be reduced. Fig.4 shows the obtained flux limit comparing with other results. Even though the detection efficiency is not good enough since 2.2 MeV is very low energy in SK (cf. the analysis threshold of solar neutrino is 3.5 MeV (kinetic)), the world best limit in below 16MeV was obtained.

In order to achieve a high detection efficiency for neutrons, it is proposed to add 0.2% of gadolinium (Gd) sulfate into SK. Since Gd has a neutron capture cross section of 49.000 barns (about 5 orders of magnitude larger than of protons) and emits a gamma cascade of 8 MeV, neutrons can be easily detected at SK.

In this context, EGADS (Evaluation Gadolinium's Action on Detector Systems) project was funded in 2009. The main motivation of EGADS is to show that by adding Gd, SK will be able to detect anti-neutrinos using the delayed coincidence technique, while keeping all its capabilities in the other analyses like solar and atmospheric neutrinos. Since then, a new hall near the SK detector has been excavated and a 200 ton tank with its ancillary equipment has been installed,

see the left of Fig.5, to mimic the conditions at SK. Of special importance is the water system, that filters out water impurities while it keeps the Gd in the water.

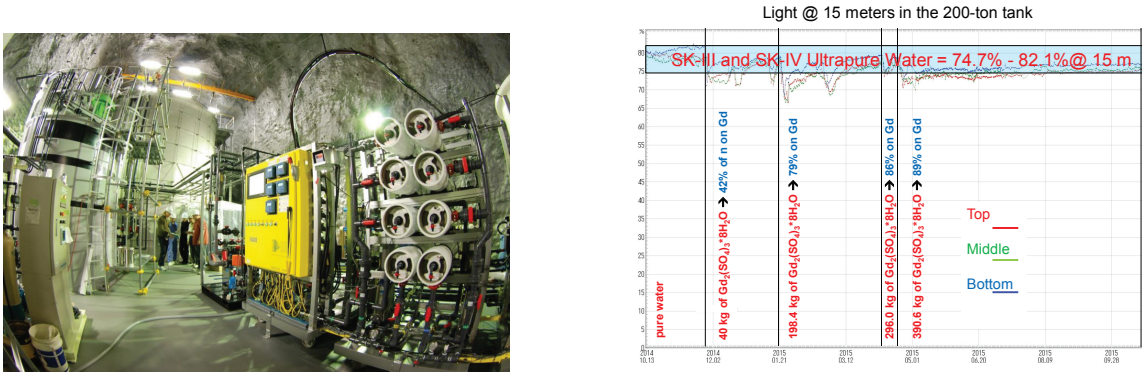

Figure 5. Left: Gd pre-mixing and pre-treatment 15 ton tank (front left), the selective filtration system (front right) and the 200 ton tank (rear of the hall). Right: Cherenkov light left at 15m for Gd loaded water. The horizontal blue band is the water transparency range of SK water. The vertical lines shows the Gd-injection date where we also indicate the concentration (% in mass) in the 200 ton tank.

From January 2010 to July 2011 pure water was circulated through the 200 ton tank and proved that the developed water system is stable and achieves a high water quality. In 2013, from February 6th to April 20th, the 200 ton tank has been step-wise loaded with Gd until the final 0.2% concentration was reached. By measuring Gd concentration at some detector positions, it was confirmed that the Gd sulfate dissolves homogeneously in the 200 ton tank, a good water quality can be maintained. In summer 2013, 240 photomultipliers were installed and the data taking has been started from September without Gd. After the water quality became good and stable, detector calibrations were performed. In April 2015, the final configuration with 0.2% $Gd_2(SO_4)_3$ concentration was achieved. The right of Fig.5 shows the time variation of Cherenkov light left at 15m for Gd loaded water. The blue band in the figure shows the transparency range of Super-K water. As shown in the figure, it is measured that the transparency of 0.2% $Gd_2(SO_4)_3$ water is 92% of the average of Super-K water.

Based on these achievements, on June 27, 2015, the SK collaboration approved the SK-Gd project which will enhance anti-neutrino detectability by dissolving gadolinium to the SK water. Detailed studies, such as PMT signal stability in Gd water, Rayleigh scattering measurement in EGADS detector, and the neutron capture efficiency are ongoing now.

References

[1] Hosaka J *et al* 2006 *Phys. Rev. D* **73** 112001
[2] Ahmad Q *et al* 2001 *Phys. Rev. Lett.* **87** 071301
[3] Mikheyev S and Smirnov A 1985 *Sov. Jour. Nucl. Phys.* **42** 913; Wolfenstein L 1978 *Phys. Rev. D* **17** 2369
[4] Smy M *et al* 2004 *Phys. Rev. D* **69** 011104(R)
[5] Renshaw A *et al* 2014 *Phys. Rev. Lett.* **112** 091805
[6] Bays K *et al* 2012 *Phys. Rev. D* **85** 052007
[7] Zhang H *et al* 2015 *Astropart. Phys.* **60** 41